Journal of Human Evolution 186 (2024) 103467

Contents lists available at ScienceDirect

Journal of Human Evolution

journal homepage: www.elsevier.com/locate/jhevol

Differences in maxillary premolar form between *Cercocebus* and *Lophocebus*

Debbie Guatelli-Steinberg [a,b,*], Kaita Gurian [a], W. Scott McGraw [a]

[a] Department of Anthropology, The Ohio State University, 174 West 18th Ave, Columbus, OH, 43210, USA
[b] School of Anthropology and Conservation, University of Kent, Canterbury, Kent, CT2 7NR, UK

ARTICLE INFO

Handling editor:Dr. C Zanolli

1. Introduction

Field observations of the sooty mangabey *Cercocebus atys* reveal that these monkeys consume hard foods year-round. (McGraw et al., 2011, 2012, 2014). Indeed, 25–80% of the *Cercocebus atys* monthly diet consists of *Sacoglottis gabonensis* seeds, which are protected by seed casings twice as hard as cherry pits (Daegling et al., 2011). By contrast, the grey-cheeked mangabey *Lophocebus albigena* relies on hard foods as dietary fallbacks, and does not eat them year-round (Lambert et al., 2004). A direct comparison of the hardness of these two species diets has yet to be made, but it is clear that the species differ in the frequency with which they consume hard foods. While fallback consumption of hard foods would be expected to select for fracture-resistance in teeth, the more frequent consumption of hard foods—as occurs in *Cercocebus atys*—would expose teeth to greater opportunity for fracture as well as increase their risk of fatigue failure (Guatelli-Steinberg et al., 2022). For these reasons, we previously hypothesized that the molars of *Cercocebus atys* would show evidence of greater resistance to fracture than those of *Lophocebus albigena* (Guatelli-Steinberg et al., 2022).

Consistent with this hypothesis, *Cercocebus atys* molars exhibit: 1) greater absolute crown strength (ACS; Schwartz et al., 2020), 2) thicker enamel in occlusal basins relative to overall enamel thickness, and 3) greater flare of cusps most directly involved in phase II of the chewing cycle (Guatelli-Steinberg et al., 2022). Schwartz et al. (2020) found that ACS—the square root of the product of average enamel thickness (AET; Martin, 1985) and half the bicervical diameter (BCD)—more closely approximates a tooth's resistance to fracture than does relative enamel thickness (RET; Martin, 1985). Proportionally thicker enamel in molar occlusal basins, where food is crushed and ground, tends to be found in hard-object feeders (Kono, 2004; O'Hara, 2021; Schwartz, 2000). Finally, flare of the lateral walls of cusps most directly involved in phase II of the chewing cycle may buttress molars against laterally directed chewing forces (Macho and Shimizu, 2009). That *Cercocebus atys* molars exhibit these features to a greater degree than those of *Lophocebus albigena* suggests that they are more fracture-resistant.

Differences in molar form between *Cercocebus* and *Lophocebu*s have only recently been described (Guatelli-Steinberg et al., 2022), while differences in the size of their premolars—specifically their P4s—were noted years ago (Fleagle and McGraw, 1999, 2002). Compared to members of the *Lophocebus–Papio* clade, species in the *Cercocebus-Mandrillus* clade are characterized by P4s that are larger relative to their M1s. Molarization of P4s is linked to the unique feeding niche of the *Cercocebus-Mandrillus* clade in which hard nuts and seeds are harvested "from the leaf litter of the forest floor" (Fleagle and McGraw, 1999: 1159). Although neither enlarged P_4s (Daegling et al., 2011) nor P^4s (Scott et al., 2018) are unique to hard-object feeders (Daegling et al., 2011; Scott et al., 2018), the P^4s of primate hard-object feeders are large relative to their M^1s (Scott et al., 2018), likely reflecting functional integration of their P^4s with their molars (Scott et al., 2018).

Field observations reveal that *Cercocebus atys* uses its P4s in concert with its molars to crush hard foods (McGraw et al., 2011). The hard seed casings are placed on the postcanine tooth row (Supplementary Online Material [SOM] Fig. S1), where they are shattered with a powerful bite (Daegling et al., 2011). Lack of significant microwear differences between the P_4s and molars of *Cercocebus atys* also suggests that these tooth types have similar functions, at least in terms of comminution (Daegling et al., 2011).

Here, using a limited maxillary dental sample, we asked whether the P^4s of *Cercocebus* (*Cercocebus atys* and *Cercocebus torquatus*) differ from those of *Lophocebus* (*Lophocebus albigena and Lophocebus aterrimus*) in ways that parallel the differences in their molars. Specifically, we predicted that compared to the P^4s of *Lophocebus*, those of *Cercocebus* would

---

* Corresponding author. Department of Anthropology, The Ohio State University, 174 West 18th Ave, Columbus OH 43210, USA.
E-mail address: guatelli-steinberg.1@osu.edu (D. Guatelli-Steinberg).

https://doi.org/10.1016/j.jhevol.2023.103467
Received 25 July 2023; Received in revised form 10 November 2023; Accepted 11 November 2023

have greater ACS, thicker occlusal basin enamel relative to AET, and greater flare of their lingual cusp walls, as lingual cusps of upper post-canine teeth are more directly involved in phase II crushing and grinding than buccal or ‘guiding’ cusps (Hillson, 1996). Finally, given known differences in molarization of the P^4s between *Cercocebus* and *Lophocebus* (Fleagle and McGraw, 1999, 2002), we predicted that the pattern of ACS change across the P^4–M^3 series would differ between the two genera, with the P^4 being most divergent.

2. Materials and methods

Specimens are listed in the SOM Table S1. Our *Cercocebus atys* specimens are from the Taï Forest of Coˆte d’Ivoire, collected by Author #3 and members of the Taï Forest Monkey Project. The specimen of *Cercocebus torquatus* is from Sette Cama Gabon and was collected by Cathy Cooke (Saint Louis University). All *Cercocebus* specimens are housed in the Primate Laboratory in the Department of Anthropology at The Ohio State University as are four of the *Lophocebus albigena* specimens. These four *Lophocebus albigena* specimens were collected by Randall Susman (Stony Brook University) near the Mambili River in the Republic of Congo (Randall Susman, pers. comm). Three of the *Lophocebus albigena* specimens and the single *Lophocebus aterrimus* specimen included here are from the American Museum of Natural History (AMNH), collected from Democratic Republic of Congo (formerly Zaire). Eric Delson and the AMNH Department of Mammalogy provided access to these data, the collection of which was funded by AMNH and New York Consortium in Evolutionary Primatology. The files were downloaded from www.MorphoSource.org, Duke University. The archival resource key (ARK) identification labels and specimen numbers of the four MorphoSource specimens are given in the SOM Table S1.

Like *Cercocebus atys* at Taï, *Cercocebus torquatus* from Sette Cama Gabon is habitually durophagous, consuming *Sacoglottis gabonensis* seeds and other hard foods year-round (Cooke, 2012). Feeding data for the *Lophocebus albigena* individuals were not collected; however, feeding data on *Lophocebus albigena* are available from Lop´e, Gabon (Ham, 1994; Tutin et al., 1997), Makande, Gabon (Brugiere et al., 2002), the Dja Reserve in Cameroon (Poulsen et al., 2001, 2002), and Uganda’s Kibale Forest (Lambert et al., 2004; Olupot, et al., 1997; Waser, 1984). At these sites, *Lophocebus albigena* prefers fruit but switches to seed-eating when fruit is scarce. There is no indication that *Lophocebus albigena* consumes hard-object foods year round. The diets of *Lophocebus aterrimus* are less well-known than those of its congener; their diets also include seeds and nuts (Horn, 1987), but whether these are fallback foods has not been documented.

Choice of right or left teeth was based on which was least worn. Where known we listed the sex of specimens in the SOM Table S1.

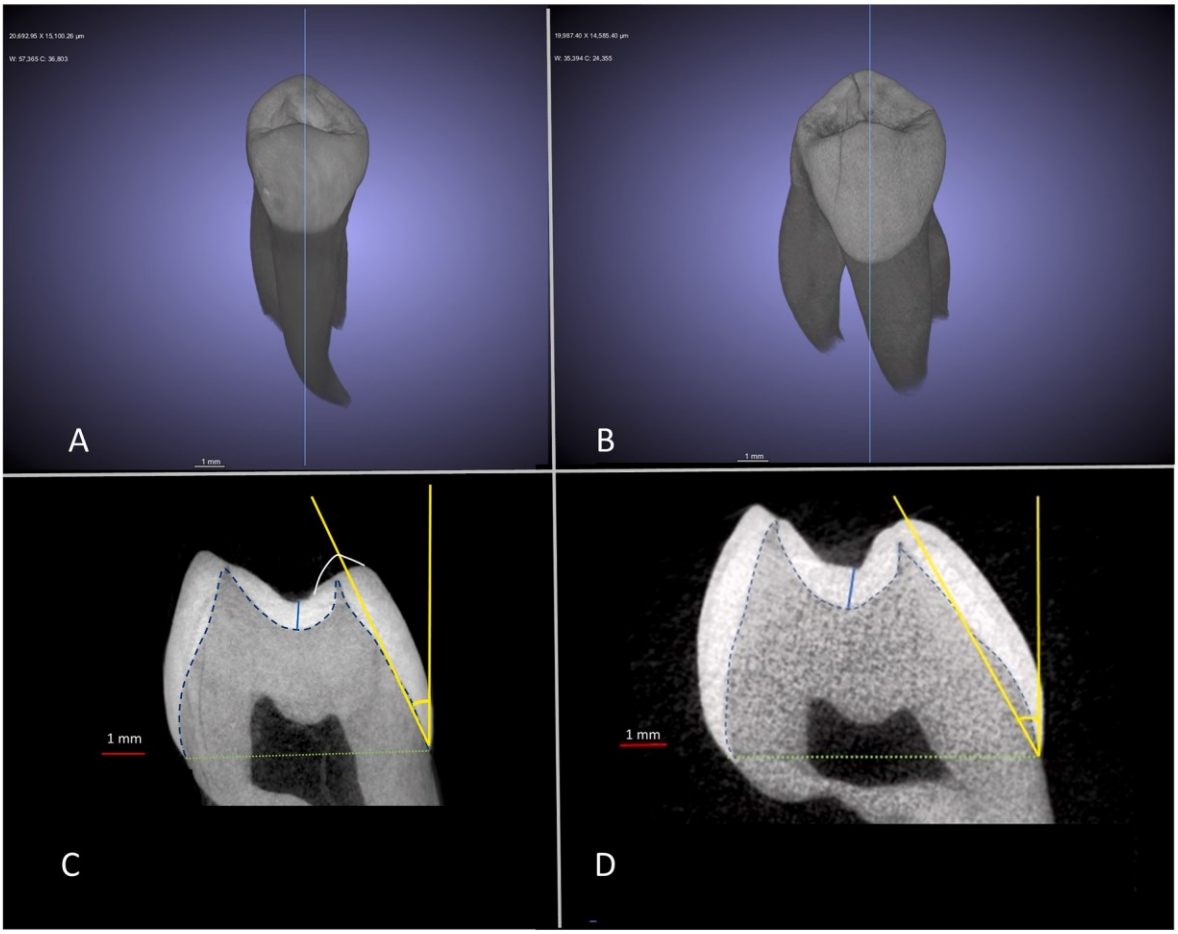

Fig. 1. *Cercocebus* and *Lophocebus* P^4 comparison with measurements reference lines. A) Three-dimensional digital rendering of the right P^4 of *Lophocebus albigena* specimen 85-7 oriented in a lingual view. The light blue line shows where the premolar was virtually sectioned. B) Three-dimensional digital rendering of the right P^4 of *Cercocebus atys* specimen 24-3 oriented in a lingual view. The light blue line shows where the premolar was virtually sectioned. C) Virtual buccolingual slice through the two P^4 cusps of *Lophocebus albigena* specimen 85-7. D) Virtual buccolingual slice through the two P^4 cusps of *Cercocebus atys* specimen 24-3. In C and D, the dotted green line represents the bicervical diameter (BCD), the dashed blue line represents the enamel-dentine junction, the solid light blue line indicates where occlusal basin linear enamel thickness was measured, and the yellow angle represents the measurement of premolar flare. Note the thicker occlusal basin enamel thickness and greater premolar flare as compared to the P^4 of *Lophocebus albigena*. (For interpretation of the references to colour in this figure legend, the reader is referred to the Web version of this article.)

Sample sizes per sex were too small for us to analyze separately, so teeth of both sexes were combined for analysis. Note that there is a large percentage of males in the *Lophocebus albigena* sample.

For specimens of Ohio State's Primate Laboratory, teeth were manually extracted from maxillae and scanned at resolutions of 13–22 μm using a Bruker Skyscan^{TM} 1172 High Resolution Ex Vivo 3D X-Ray Tomography Scanner. Raw output files were processed with N.Recon v. 1.7.4.2 (Bruker MicroCT, Kontich) and saved as Tif files. The four AMNH specimens were scanned by Eric Delson (American Museum of Natural History and Lehman College-City University of New York) and downloaded from MorphoSource, with resolutions ranging from 61 to 75 μm. For premolars, two-dimensional (2D) buccolingual planes of section, passing through buccal and lingual dentine horns and perpendicular to the cervical margin (Fig. 1) were generated from three-dimensional digital renderings (following Skinner et al., 2015) using Dragonfly v. 2021.1.0.977 (Object Research Services, Montréal). Similar 2D sections were generated from molar three-dimensional renderings, with section planes passing through mesial cusps. Virtual sections were saved as Tif files and imported into Adobe Photoshop v. 22.2 (Microsoft, San Jose), where crown outlines were reconstructed (when necessary) prior to performing measurements (see below).

Fig. 1 depicts measurement reference points and lines. Average enamel thickness was calculated as the enamel cap area divided by enamel-dentine junction length (Martin, 1985). Absolute crown strength was calculated as the square root of the product of the coronal dentine radius (half of the BCD) and AET (Schwartz et al., 2020). Linear enamel thickness of the occlusal basin was measured as the distance between the lowest point of the occlusal basin at the enamel-dentine junction and the lowest point of the occlusal basin at the outer enamel surface (Kono-Takeuchi et al., 1998). Linear occlusal basin thickness was divided by AET to obtain proportional linear occlusal basin thickness (pLOB; O'Hara, 2021); values greater than one represent thicker enamel in the occlusal basin relative to the average enamel thickness of a molar (Guatelli-Steinberg et al., 2022; O'Hara, 2021). To measure cusp flare, a reference line was first drawn perpendicular to the BCD. Then, a second reference line was drawn from the cemento-enamel junction to the cusp tip (or reconstructed cusp tip). The angle included between the two references lines quantifies cusp flare (Shimizu, 2002). Measurements were made by the first two authors, whose inter-observer measurement error was assessed (SOM Table S2).

Worn crowns were reconstructed following recommendations of O'Hara and Guatelli-Steinberg (2021) using either 'Profile' or 'Pen Tool' methods. The Profile method involves completing worn portions of enamel cusps and dentine horn tips using outer enamel surface curvature profiles of unworn teeth of the same tooth type (Smith et al., 2011). The Pen Tool method makes use of Adobe Photoshop's 'Pen Tool' to find the intersection of the two sides of the worn cusp, creating a rounded shape representing the unworn cusp tip (Saunders et al., 2007; Guatelli-Steinberg et al., 2009; O'Hara et al., 2019).

O'Hara and Guatelli-Steinberg (2021) found that for AET and crown height measurements, when wear did not reach the dentine horns and/or the deepest point of occlusal basins, accurate values were achievable with both the Profile and Pen Tool methods. O'Hara and Guatelli-Steinberg (2021) also found that for crowns on which wear exposed dentine horn tips (what they termed 'extensive wear'), it was possible to obtain accurate AET values using the Profile method. Following the recommendations of O'Hara and Guatelli-Steinberg (2021), the Profile method was used for AET and cusp flare on teeth with extensive wear. The Pen Tool method was used if a reference tooth was not available but wear did not breach the dentine horn. Measurements of enamel thickness in occlusal basins were only made on teeth with unworn occlusal basins.

One-tailed t-tests were used to compare *Cercocebus* and *Lophocebus* for ACS and premolar flare. These variables were normally distributed. Because a Shapiro-Wilks test revealed that pLOB was not normally distributed, a Mann-Whitney U test was used to compare the two genera for this variable. Spearman correlation coefficients were calculated among the three variables. These tests were performed in SAS v. 9.4 (SAS Institute, Cary).

To analyze the pattern of ACS change across the P^4–M^3 series, statistical analyses were conducted in SAS using the mixed procedure (Proc Mixed). This procedure fits mixed linear models to data, allowing a repeated measures analysis of molars belonging to the same individuals and accommodating missing data. Fixed effects for genus, tooth type and their interaction were obtained. Given differences in molarization of the P^4 between the two genera, we predicted that there would be a significant interaction effect between genus and tooth type.

3. Results

The *t*-test for a difference in the means of P^4 ACS between *Cercocebus* and *Lophocebus* was statistically significant ($t = 7.337$, $df = 13.850$, $p < 0.000$), with *Cercocebus* greater than *Lophocebus*. A Mann-Whitney U test used to test for a difference in the central tendencies of P^4 pLOB for *Cercocebus* and *Lophocebus* indicated a statistically significant difference between the two genera, with *Cercocebus* greater than *Lophocebus* ($U = 47.0$; Chi-square approximation $= 4.835$, $df = 1$, $p < 0.028$). For P^4 flare, a one-tailed *t*-test revealed a statistically significant difference between *Cercocebus* and *Lophocebus* ($t = 2.2$, $df = 11.521$, $p < 0.022$), again with the *Cercocebus* mean exceeding that of *Lophocebus*.

None of the Spearman correlations among the three variables ACS, pLOB and flare were statistically significant across the entire P^4 sample (see SOM Table S3) suggesting a degree of independence among these three variables (although larger samples might reveal correlations that are significant). Means and standard deviations for P^4 ACS, pLOB and flare for each genus and species are given in Table 1. Box plots of these three variables as well as for AET and BCD, are shown in Fig. 2. These distribution plots reveal that there is greater separation between the two genera for BCD, a measure of tooth size, than there is for AET. Because ACS is the product of crown radius and AET, these plots suggest that the differences in ACS between the two genera are more a function of differences in tooth size than AET.

Results of the repeated measures linear regression analysis for ACS are given in Table 2. Analysis of the residuals from the regression suggest that they were normally distributed (SOM Fig. S2). There were statistically significant differences between the two genera as well as among the four different tooth types. The interaction between genus and tooth type was not statistically significant, but the plot of estimated least squares means in Fig. 2 suggests that the greatest difference between these two genera in the pattern of ACS change across tooth types occurs between P^4 and M^1.

Table 1
Maxillary fourth premolar descriptive statistics, including means and standard deviations.

Taxa	BCD ±1 SD (*n*)	AET ± 1 SD (*n*)	ACS ± 1 SD (*n*)	pLOB ± 1 SD (*n*)	Flare ± 1 SD (*n*)
Cercocebus atys	6.74 ± 0.58 (7)	0.650 ± 0.068 (7)	1.48 ± 0.09 (7)	1.32 ± 0.22 (7)	23.47 ± 4.59 (7)
Cercocebus torquatus	6.46 (1)	0.711 (1)	1.52 (1)	–	22.50 (1)
All *Cercocebus*	6.71 ± 0.55 (8)	0.658 ± 0.067 (8)	1.48 ± 0.08 (8)	1.32 ± 0.22 (7)	23.35 ± 4.26 (8)
Lophocebus albigena	5.12 ± 0.51 (7)	0.571 ± 0.041 (7)	1.21 ± 0.08 (7)	1.13 ± 0.10 (7)	18.86 ± 2.26 (7)
Lophocebus aterrimus	5.26 (1)	0.521 (1)	1.17 (1)	1.18 (1)	23.12 (1)
All *Lophocebus*	5.14 ± 0.47 (8)	0.565 ± 0.042 (8)	1.20 ± 0.072 (8)	1.14 ± 0.10 (8)	19.39 ± 2.58 (8)

Abbreviations: BCD = bicervical diameter (in mm); AET = average enamel thickness (in mm); ACS = absolute crown strength (mm); pLOB = proportional linear occlusal basin thickness (unitless ratio); Flare = premolar cusp flare (in degrees).

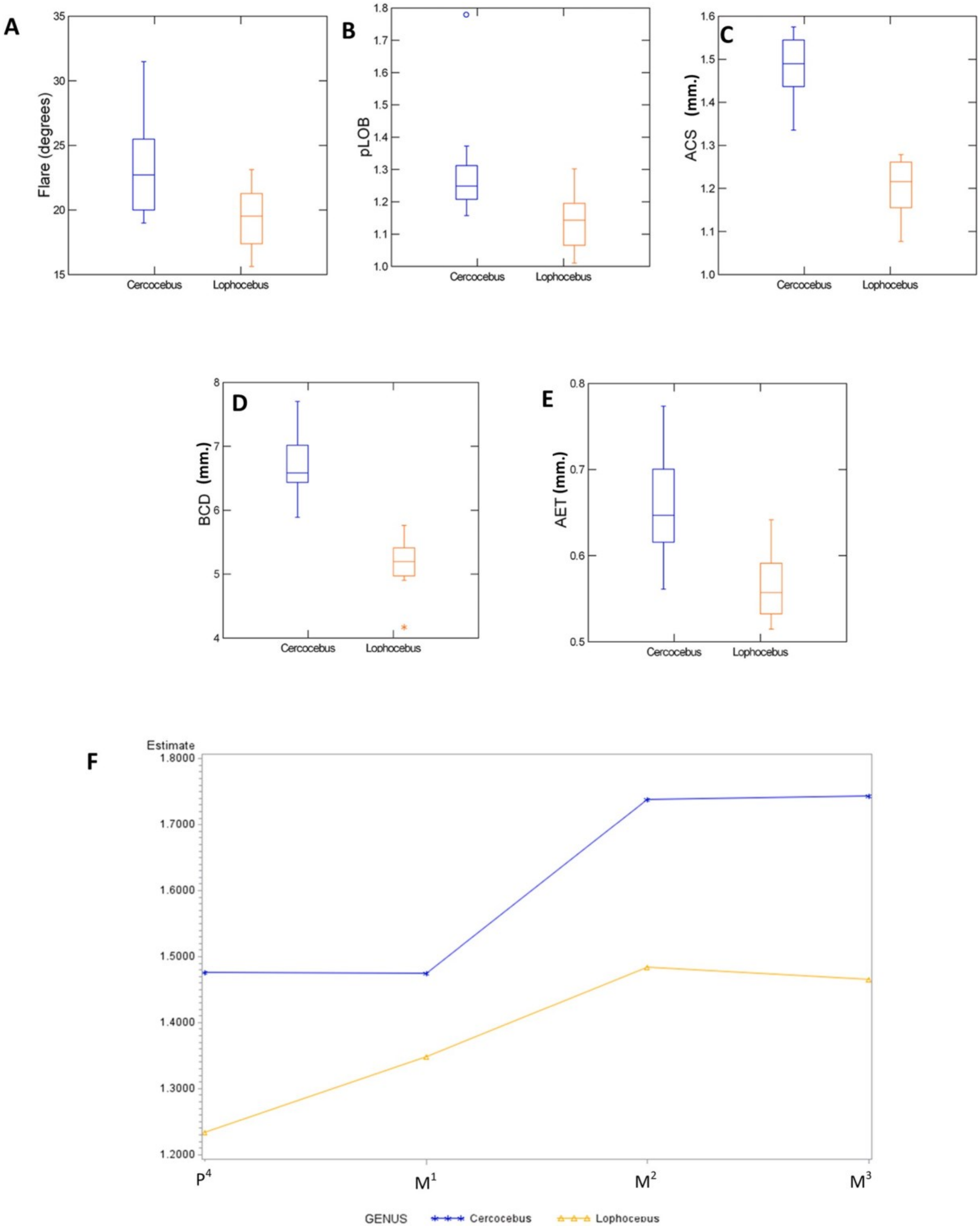

Fig. 2. Graphical representation of data and plot of least squares means. Box plots of premolar flare (A), proportional linear occlusal basin enamel thickness (pLOB; B), absolute crown strength (ACS; C), bicervical diameter (BCD; D), and absolute enamel thickness (AET; E). Note the greater values for *Cercocebus* as compared to *Lophocebus* for ACS, and the greater values for *Cercocebus* in BCD length. F) Least squares estimates from the linear regression of ACS on molar type by species. Note that the estimate for the *Cercocebus* P^4 is similar to that of its M^1.

4. Discussion and conclusions

Here, the P^4 crowns of *Cercocebus* and *Lophocebus* were compared with respect to ACS, pLOB enamel thickness, and the flare of their lingual cusp lateral walls. Based on known differences in the molar form of these two genera (Guatelli-Steinberg et al., 2022), all three features were expected to have greater values in *Cercocebus* relative to *Lophocebus*. Results of our analysis confirm these expectations. *Cercocebus* P^4s thus share with their molars features affording them greater resistance to fracture than do the P^4s and molars of *Lophocebus*.

Although there was no statistically significant interaction between tooth type and genus, plots of estimated least squares means from this regression (Fig. 2) suggest that ACS of the P^4 and M^1 are more similar to each other in *Cercocebus* than they are in *Lophocebus*. We caution that the

Table 2
Type 3 tests of fixed effects for repeated measures linear regression.[a]

Effect	Degrees of freedom in numerator	Degrees of freedom in denominator	F value	*P*-value
Tooth type (P^4–M^1–M^2–M^3)	3	16	50.57	**<0.0001**
Genus (*Cercocebus*–*Lophocebus*)	1	9	20.21	**0.0014**
Interaction of tooth type and genus	3	16	1.19	0.3435

[a] Significant p-values are highlighted in bold.

present study included only a single M^1 for *Cercocebus atys*. However, average P^4 ACS of *Cercocebus* calculated in this study is 1.49 ($n = 8$), while average M^1 ACS of *Cercocebus* reported in Guatelli-Steinberg et al. (2022) is 1.48 ($n = 7$). These average ACS values for *Cercocebus* P^4 and M^1 are quite close. By contrast, the P^4 ACS average for *Lophocebus* reported here is 1.20 ($n = 8$), representing a 13.7% decrease from the *Lophocebus* M^1 ACS average of 1.39 ($n = 4$) reported in Guatelli-Steinberg et al. (2022). Because ACS is a product of both the size of the crown (specifically crown radius) and its AET, this result is an expected consequence of known differences in P^4 molarization between these two genera (Fleagle and McGraw, 1999, 2002).

Three caveats regarding the present study merit comment. First, we did not correct for multiple statistical comparisons owing to small sample sizes, which limit the power of our statistical tests and increase the probability of type II error. A Bonferroni-corrected alpha for three separate P^4 comparisons (of ACS, pLOB and flare), would be 0.0017, and if applied here would result in only the ACS p-value falling below this critical value. Second, seven of eight of individuals in our *Lophocebus* sample were male. What effect this might have on comparisons is not clear, although if male crowns tend to be larger than those of females, then we might expect ACS differences between *Cercocebus* and *Lophocebus* to be even greater in comparisons with more equal representation of males and females. Third, this study relates premolar form to current dietary differences between *Cercocebus* and *Lophocebus*. We do not know how far back in time these dietary differences extend, which would be relevant for evaluating adaptive hypotheses, as would a broader understanding of molar form as it relates to diet in the diverse extant members of the *Cercocebus-Mandrillus* and *Papio-Lophocebus* clades. Further investigation is clearly needed to address these complex questions.

Scott et al. (2018) found that the premolars of primate hard object feeders are large relative to their M^1s but not relative to their mandibular lengths, the latter of which these authors used as an indicator of load resistance and force production. They suggested that this finding "… challenges the idea that hard-object feeders have enlarged premolars as an adaptive response to resisting loads incurred when processing mechanically challenging foods" (Scott et al., 2018: 221). Instead, Scott et al. (2018: 221) argued, the large P^4/M^1 ratios of hard-object feeders are more likely to reflect "… greater functional integration across the premolar-molar boundary owing to a mesial shift in the bite point."

It is not clear whether the differences found here in P^4 ACS, pLOB, and flare of *Cercocebus* relative to *Lophocebus* reflect differences in their bite points, differences in the frequency of hard food consumption, differences in force production, or some combination of these factors. Deutsch et al. (2020) found *Cercocebus atys* to have the highest estimated bite force among 23 comparative primate species (Deutsch et al., 2020), including much larger-bodied mandrills. Consistent with its high bite force, *Cercocebus atys* also has a high P^4 to mandibular length ratio (Fannin et al., 2021), suggesting that its enlarged fourth premolars are (at least in part) related to load resistance.

Study of the P^4 crown features described here, along with the P4/M1 ratio itself, might provide further insight into the degree to which fossil papionins such as *Procercocebus* (Gilbert, 2007) relied upon hard-object foods. Insofar as it is possible to assess the nature of hard object feeding in fossil taxa, we note that *Cercocebus* and *Lophocebus* differ in both premolar (present study) and molar form (Guatelli-Steinberg et al., 2022). Clear differences in posterior tooth form between *Cercocebus* and *Lophocebus* strongly suggest that fallback and habitual consumption of hard foods are not necessarily associated with the same dental features. This realization may be useful in inferring the nature of hard object feeding in fossil taxa.

Acknowledgments

Funded by NSF grant 1945008. The authors thank Mackie O'Hara, Gary Schwartz, and Leigh Oldershaw for productive discussions and contributions to grant proposal preparation. We thank our undergraduate tooth extraction team: Gina De Marsh, Ryan Phelan, Jess Rychel, and Ellie Sarle. Special thanks to Jie Liu for her advice and assistance with µCT scanning and to Do-Gyoon Kim for use of the scanner in his lab. We thank Brian Foster and Michael Chavez for an introduction to µCT scanning.

Supplementary Online Material

Supplementary Online Material to this article can be found online at https://doi.org/10.1016/j.jhevol.2023.103467.

References

Brugiere, D., Gautier, J.-P., Moungazi, A., Gautier-Hion, A., 2002. Primate diet and biomass in relation to vegetation composition and fruiting phenology in a rain forest in Gabon. Int. J. Primatol. 23, 999–1024.

Cooke, C.A., 2012. The feeding, ranging, and positional behaviors of *Cercocebus torquatus*, the red-capped mangabey in Sette Cama Gabon: A Phylogenetic Perspective. In: . Ph.D. Dissertation, The Ohio State University.

Daegling, D.J., McGraw, W.S., Ungar, P.S., Pampush, J.D., Vick, A.E., Bitty, E.A., 2011. Hard-object feeding in sooty mangabeys (*Cercocebus atys*) and interpretation of early hominin feeding ecology. PLoS One 6, e23095.

Deutsch, A.R., Dickinson, E., Leonard, K.C., Pastor, F., Muchlinski, M.N., Hartstone-Rose, A., 2020. Scaling of anatomically derived maximal bite force in primates. Anat. Rec. 303, 2026–2035.

Fannin, L.D., Guatelli-Steinberg, D., Arft-Guatelli, J., Dunham, N.T., Traff, J.E., Palvadore, T., Donaldson, A., Cunneyworth, P., Daegling, D.J., McGraw, W.S., 2021. Oral processing, folivory, and premolar size in eight cercopithecoid monkeys. Am. J. Phys. Anthropol. 174 (Suppl. 71), 30.

Fleagle, J.G., McGraw, W.S., 1999. Skeletal and dental morphology supports diphyletic origin of baboons and mandrills. Proc. Natl. Acad. Sci. USA 96, 1157–1161.

Fleagle, J.G., McGraw, W.S., 2002. Skeletal and dental morphology of African papionins: unmasking a cryptic clade. J. Hum. Evol. 42, 267–292.

Gilbert, G.S., 2007. Craniomandibular morphology supporting the diphyletic origin of mangabeys and a new genus of the *Cercocebus/Mandrillus* clade, *Procercocebus*. J. Hum. Evol. 53, 69–102.

Guatelli-Steinberg, D., Ferrell, R.J., Spence, J., Talabere, T., Hubbard, A., Schmidt, S., 2009. Sex differences in anthropoid mandibular canine lateral enamel formation. Am. J. Phys. Anthropol. 140, 216–233.

Guatelli-Steinberg, D., Schwartz, G.T., O'Hara, M.C., Gurian, K., Rychel, J., McGraw, W. S., 2022. Molar form, enamel growth, and durophagy in *Cercocebus* and *Lophocebus*. Am. J. Biol. Anthropol. 179, 386–404.

Ham, R.M., 1994. Behaviour and Ecology of Grey-Cheeked Mangabeys (*Cercocebus Albigena*) in the Lope Reserve, Gabon. Ph.D. Dissertation,. University of Stirling.

Hillson, S., 1996. Dental Anthropology. Cambridge University Press, Cambridge.

Horn, A.D., 1987. The socioecology of the black mangabey (*Cercocebus aterrimus*) near Lake Tumba, Zaire. Am. J. Primatol. 12, 165–180.

Kono, R.T., 2004. Molar enamel thickness and distribution patterns in extant great apes and humans: new insights based on a 3-dimensional whole crown perspective. Anthropol. Sci. 112, 121–146.

Kono-Takeuchi, R., Suwa, G., Kanazawa, E., Tanijiri, T., 1998. A new method of evaluating enamel thickness based on a three-dimensional measuring system. Anthropol. Sci. 105, 217–229.

Lambert, J.E., Chapman, C.A., Wrangham, R.W., N.L. Conklin-Brittain, N.L., 2004. Hardness of cercopithecine foods: implications for the critical function of enamel thickness in exploiting fallback foods. Am. J. Phys. Anthropol. 125, 363–368.

Macho, G.A., Shimizu, D., 2009. Dietary adaptations of South African australopiths: inference from enamel prism attitude. J. Hum. Evol. 57, 241–247.

Martin, L., 1985. Significance of enamel thickness in hominoid evolution. Nature 314, 260–263.

McGraw, W.S., Vick, A.E., Daegling, D.J., 2011. Sex and age differences in the diet and ingestive behaviors of sooty mangabeys (*Cercocebus atys*) in the Tai Forest, Ivory Coast. Am. J. Phys. Anthropol. 144, 140–153.

McGraw, W.S., Pampush, J.D., Daegling, D.J., 2012. Brief Communication: Enamel thickness and durophagy in mangabeys revisited. Am. J. Phys. Anthropol. 147, 326–333.

McGraw, W.S., Vick, A.E., Daegling, D.J., 2014. Dietary variation and food hardness in sooty mangabeys (*Cercocebus atys*): implications for fallback foods and dental adaptation. Am. J. Phys. Anthropol. 154, 413–423.

O'Hara, M.C., 2021. Features of catarrhine posterior dental crowns associated with durophagy: Implications for fossil hominins. Ph.D. Dissertation, The Ohio State University.

O'Hara, M.C., Guatelli-Steinberg, D., 2021. Reconstructing tooth crown heights and enamel caps: a comparative test of three existing methods with recommendations for their use. Anat. Rec. 305, 123–143.

O'Hara, M.C., Le Cabec, A., Xing, S., Skinner, M.F., Guatelli-Steinberg, D., 2019. Safe casting and reliable cusp reconstruction assisted by micro-computed tomographic scans of fossil teeth. Anat. Rec. 302, 1516–1535.

Olupot, W., Chapman, C.A., Waser, P.M., Isabirye-Basuta, G., 1997. Mangabey (*Cercocebus albigena*) ranging patterns in relation to fruit availability and the risk of parasite infection in Kibale National Park, Uganda. Am. J. Primatol. 43, 65–78.

Poulsen, J.R., Clark, C.J., Smith, T.B., 2001. Seasonal variation in the feeding ecology of the grey-cheeked mangabey (*Lophocebus albigena*) in Cameroon. Am. J. Primatol. 54, 91–105.

Poulsen, J.R., Clark, C.J., Connor, E.F., Smith, T.B., 2002. Differential resource use by primates and hornbills: implications for seed dispersal. Ecology 83, 228–240.

Saunders, S.R., Chan, A.H., Kahlon, B., Kluge, H.F., FitzGerald, C.M., 2007. Sexual dimorphism of the dental tissues in human permanent mandibular canines and third premolars. Am. J. Phys. Anthropol. 133, 735–740.

Schwartz, G.T., 2000. Taxonomic and functional aspects of the patterning of enamel thickness distribution in extant large-bodied hominoids. Am. J. Phys. Anthropol. 111, 221–244.

Schwartz, G.T., McGrosky, A., Strait, D.S., 2020. Fracture mechanics, enamel thickness and the evolution of molar form in hominins. Biol. Lett. 16, 20190671.

Scott, J.E., Campbell, R.M., Baj, L.M., Burns, M.C., Price, M.S., Sykes, J.D., Vinyard, C.J., 2018. Dietary signals in the premolar dentition of primates. J. Hum. Evol. 121, 221–234.

Shimizu, D., 2002. Functional implications of enamel thickness in the lower molars of red colobus (*Procolobus badius*) and Japanese macaque (*Macaca fuscata*). J. Hum. Evol. 43, 605–620.

Skinner, M.M., Alemseged, Z., Gaunitz, C., Hublin, J.J., 2015. Enamel thickness trends in Plio-Pleistocene hominin mandibular molars. J. Hum. Evol. 85, 35–45.

Smith, T.M., Bacon, A.-M., Demeter, F., Kullmer, O., Nguyen, K.T., de Vos, J., Wei, W., Zermeno, J.P., Zhao, L., 2011. Dental tissue proportions in fossil orangutans from mainland Asia and Indonesia. Hum. Orig. Res. 1, 1–6.

Tutin, C.E., Ham, R.M., White, L.J., Harrison, M.J., 1997. The primate community of the Lop´e Reserve, Gabon: diets, responses to fruit scarcity, and effects on biomass. Am. J. Primatol. 42, 1–24.

Waser, P.M., 1984. Ecological differences and behavioral contrasts between two mangabey species. In: Rodman, P.S., Cant, J.G.H. (Eds.), Adaptations for Foraging in Nonhuman Primates. Columbia University Press, New York, pp. 195–216.